Deep Downhole Seismic Testing Using a Hydraulically-Operated, Controlled-Waveform Vibroseis

K.H. Stokoe, II[1], S. Hwang[2], J.N. Roberts[3], F.M. Menq[4], A.K. Keene[5], R.C. Lee[6] and B. Redpath[7]

[1] *Professor; Jennie C. and Milton T. Graves Chair in Engineering, Department of Civil, Architectural and Environmental Engineering, University of Texas at Austin, U.S.A., k.stokoe@mail.utexas.edu*

[2] *Graduate Research Assistant, Civil, Architectural, and Environmental Engineering Department, University of Texas at Austin, U.S.A., syongmoon@utexas.edu*

[3] *Graduate Research Assistant, Civil, Architectural & Environmental Engineering Department, University of Texas at Austin, U.S.A., jnroberts@utexas.edu*

[4] *Research Associate, Department of Civil, Architectural and Environmental Engineering, University of Texas at Austin, U.S.A., fymenq@utexas.edu*

[5] *Graduate Research Assistant, Civil, Architectural, and Environmental Engineering Department, University of Texas at Austin, U.S.A., akkeene@utexas.edu*

[6] *Engineering Seismologist, Los Alamos National Laboratory, New Mexico, U.S.A., rclee@lanl.gov*

[7] *Independent Geophysicist, Redpath Geophysics, U.S.A., redpathgeophysics@gmail.com*

Abstract

Downhole seismic testing is one field test that is commonly used to determine constrained compression-wave (P) and shear-wave (S) velocity profiles in geotechnical earthquake engineering investigations. Traditional downhole testing has generally involved profiling in the 30- to 200-m depth range using hand-operated or small, mechanically-assisted sources. As the number of field investigations at locations with critical facilities has increased, profiling depths have also increased. An improved downhole test for P- and S-wave velocity profiling to depths exceeding 400 m is presented. The improvements include: (1) a more powerful source, (2) generation of simple sinusoidal waveforms, (3) the ability to "tune" the sinusoidal waveform to site conditions and (4) high-fidelity, post-processing of the time-domain records to increase signal-to-noise ratios at deeper depths. The seismic source is a large, hydraulically-operated, triaxial vibroseis named T-Rex that generates both P (vertically shaking) and S (horizontal shaking) waves. The test procedure and signal processing are discussed. Examples of raw and processed time-domain records, P- and S-wave travel-time plots, and interpreted wave velocity profiles measured to a depth of 415 m in one borehole are shown. Comparisons are also made with traditional downhole testing performed to a depth of 183 m in the same borehole.

Keywords: Field Seismic Testing, Downhole Test, Deep P- and S-Wave Profiling, Controlled Triaxial Source

1. Introduction

The downhole seismic method was employed to determine constrained compression-wave (P-wave) and shear-wave (S-wave) velocity profiles at an existing borehole at the Los Alamos National Laboratory (LANL) in New Mexico, USA. Traditional downhole testing with hand-operated impulsive sources was used to perform P- and S-wave measurements at depths from 18 to183 m. At depths from 153 to 415 m in the borehole, a large, hydraulically-operated vibroseis named T-Rex was used as a controlled-waveform source. In all measurements, a single, orientable, 3-D borehole geophone and associated wireline system were used to monitor stress wave motions at depth. In this paper, seismic sources, test procedures and signal processing are discussed. Examples of raw and processed time-domain records, P- and S-wave travel-time plots, and interpreted wave velocity profiles to a depth of 415 m are presented. Two alternative interpretations of the P- and S-wave velocity profiles are also discussed.

2. Generalized Field Arrangement for Deep Downhole Testing

The generalized setup used in downhole seismic testing at the LANL site is illustrated in Fig.1. A listing of the equipment, with brief descriptions, is presented in Table 1. The generalized setup involved two types of seismic sources. The first source type was conventional hand-operated mechanical sources that generated transient impulses to create P and S waves at the ground surface. (See item #1 in Fig.1 and in Table 1.) Vertical, sledge-hammer blows to a circular, hard-plastic plate were used to generate P waves. Shear waves were created with horizontal, sledge-hammer blows to a horizontal wooden plank with steel end caps upon which a large vertical
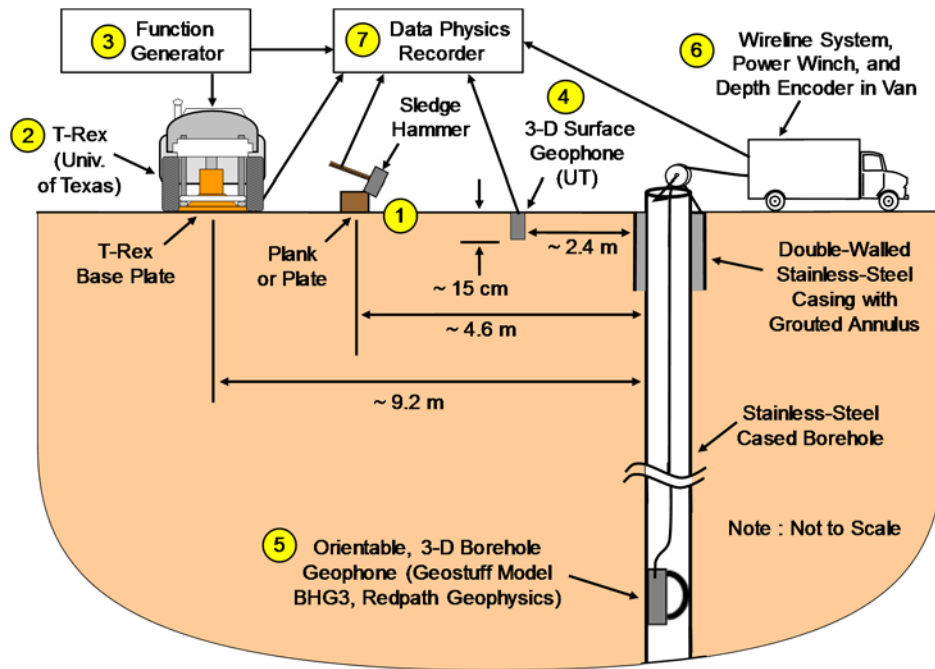
Fig. 1– Generalized field setup for downhole seismic measurements at the LANL site (Note: items in Fig.1 are described in Table 1.).

Table 1 - Listing of types, functions, and important characteristics of equipment used to perform downhole seismic measurements at the LANL site.

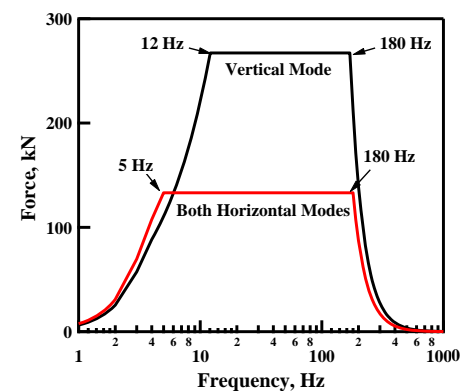| Number in Fig.1.	Equipment Type	Functions	Important Characteristics
1	Hand-Operated Seismic Sources	Transiently Generate P and S Waves	7.3-kg sledge hammer used as impact source; Geometric hammer switch for triggering Data Physics analyzer; P waves generated by vertically striking a plate (~0.3-m diam.); S waves generated by horizontally striking ends of plank loaded by pick-up truck.
2	Hydraulically-Operated, Triaxial Seismic Source, T-Rex	Generate Frequency-Controlled, P and S Waves	Off-road buggy; 9.8-m long, 2.4-m wide, 30,390 kg; 3 vibrational orientations; push-button transformation of shaking orientation; 13-kN shear mode peak force; 267-kN vertical mode peak force.
3	Function Generator	Supply Sinusoidal Drive Signal to T-Rex	Agilent 33220A Function / Arbitrary Waveform Generator; freq ≤ 20 MHz sine waveforms.
4	3-D Surface Geophone	Monitor P and S Waves at the Surface for Triggering Purposes	Three, Geospace GS-11D geophones embedded in 6.4-cm diameter, 10.2-cm tall acrylic cylinder to create a 3-component, 10-Hz surface sensor (supplied by Univ. of Texas).
5	3-D Borehole Geophone	Monitor P and S Waves at Depth for Velocity Determinations	Geostuff Model BHG3 triaxial downhole sensor, with locking mechanism and orientation system (supplied by Redpath Geophysics).
6	Wireline System in Van	Used to Lower and Raise 3-D Borehole Geophone	Electrically-operated winch with optical encoder and digital readout for measuring sensor depth.
7	Data Physics Recorder	Record and Analyze all Seismic Signals	16-channel Data Physics recorder; 97 kHz Bandwidth Mobilyzer; 24-bit input and output channels; simultaneous sampling.

static load was applied. As typically done in S-wave testing, two sets of S-wave records were collected, with the polarity of the shear wave reversed between each set of records by hitting the plank in the opposite direction. Also, signal averaging in the time domain was performed using 3 to about 10 averages in both the P- and S-wave measurements. The manually-operated sources were used over the depth range of 18 to 183 m. No downhole testing was performed at depths less than 18 m because the borehole was cased with a double-walled, stainless steel casing in this depth range which greatly inhibited stress-wave transmission.

The second type of downhole seismic source used at the LANL site was a large hydraulically-operated machine called a vibroseis in the geophysical exploration industry. The vibroseis used in this study is unique in that it is a large triaxial vibrator, meaning that it is capable of generating ground motions in the vertical and both horizontal directions. This triaxial vibroseis, named T-Rex and operated by the University of Texas at Austin (UT), functioned as a high-energy, controlled-waveform shaker. (See item #2 in Fig.1 and in Table 1.) A photograph of T-Rex is presented in Fig.2a. T-Rex weighs about 30,400 kg. The theoretical peak force outputs of T-Rex in the vertical and horizontal directions are presented in Fig.2b. When used as the seismic source, T-Rex was located on the ground surface at a fixed position about 9.2 m from the borehole. At this position, T-Rex was oriented with its longitudinal axis tangent to an imaginary circle centered at the borehole. Compression waves were generated by vertically exciting the base plate. Shear waves were generated by horizontally exciting the base plate in a direction perpendicular to a radial line from the borehole to the source. As a result, the horizontal direction of shaking had the same orientation as the hand-operated, S-wave source. In each shaking mode, the base plate was excited for a given number of cycles at a fixed frequency using a waveform function generator. The function generator is denoted as item #3 in Fig.1 and in Table 1.

For most downhole testing with T-Rex, a 50-Hz sinusoidal drive signal was used. The drive signal had 10 full-amplitude cycles and 3, tapered-amplitude cycles at the beginning and at the end of the full-amplitude cycling. The drive frequency of 50 Hz was selected in the field to optimize the P and S waveforms. This procedure was done by viewing the output from the borehole receiver during data collection. Downhole testing began with a 50-Hz drive signal and then was changed to 30 Hz at a depth of 360 m. This change in frequency was done to increase wavelength and thus decrease attenuation which resulted in improved waveform quality at the deeper depths. As done in the S-wave measurements with the sledge-hammer and plank source, two sets of S-wave records were collected, with the polarity of the shear wave reversed between the record sets by inverting the drive signal to T-Rex. Also, signal averaging was performed in the time domain for both P- and S-wave measurements. Signal averaging involved using 3 to 10 averages, with 3 averages often used. The T-Rex source was used over the depth range of 153 to 415 m. In addition, P- and S-wave measurements were performed with both hand-operated and hydraulically-operated sources at depths of 153 to 183 m for comparison purposes.

| (a) Photograph of triaxial vibrator named T-Rex | (b) Peak force outputs of T-Rex |

Fig. 2 – Triaxial vibrator, named T-Rex, that was used as a high-energy, controllable-waveform downhole source at the LANL site (from Stokoe et al, 2008 [1]).

(a) Output signals at a depth of 158 m   (b) Output signals at a depth of 293 m
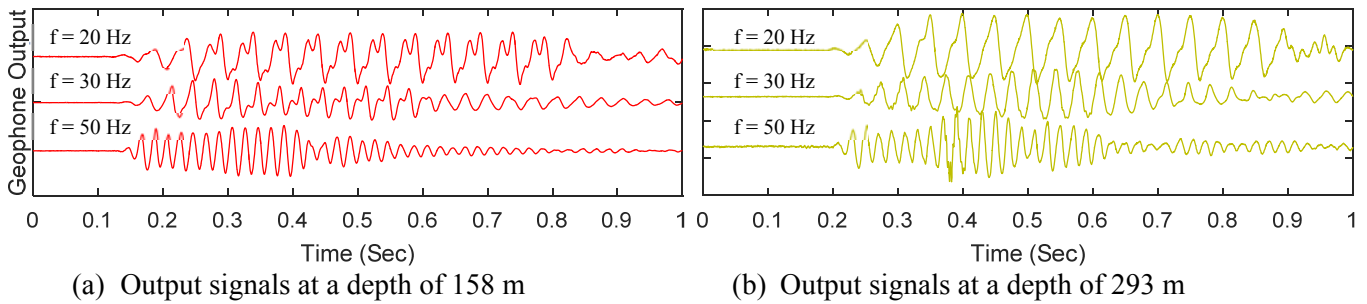
Fig. 3 – Examples in variability of sinusoidal P waveforms created using T-Rex at frequencies of 20, 30 and 50 Hz; Measurements at depths of 158 and 293 m with the vertical component in the 3-D borehole geophone.

As an example of optimizing the sinusoidal drive signal in the field, consider the P-wave records in Fig.3. All P-wave records in Fig.3 were filtered to improve clarity using a 1000-Hz, low-pass filter. In Fig.3a, sinusoidal signals generated using T-Rex shaking at three different frequencies (50, 30 and 20 Hz) are presented. The P-wave records are from measurements at a depth of 158 m. As seen in Fig.3a, the simplest waveform to analyze was created by driving T-Rex with a 50-Hz signal. On the other hand, as the depth in the borehole increased, the clarity in the P waveform at lower frequencies improved as shown in Fig.3b. In this case, the P-wave records are from a depth of 293 m, and both the 50- and 30-Hz records are clear. However, the 50-Hz measurements were continued until a depth of 360 m when the frequency was reduced to 30 Hz.

3. Monitoring the Consistency of Triggering the Seismic Sources

It is important that the triggering signal to the seismic recorder (Data Physics recorder identified as item #7 in Fig.1 and in Table 1) occurs at the same relative time for all measurement depths when using only one, 3-D borehole receiver. This triggering time is often referred to as "time zero" on each seismic record captured with the borehole receiver. This type of measurement is termed a direct, source-to-receiver measurement. The consistency in triggering when using a single borehole receiver is required to assure that the time determined between different measurement depths represents only the wave travel time between those depths and does not include other time resulting from inconsistent triggering. The actual time of triggering should be nearly constant, with a standard deviation that is small relative to some measure of the travel time at all testing depths or within each set of P- and S-waves measurements used to determine average P- and S-wave velocities for constant-velocity layers. The consistency in triggering ranged from very good to excellent as briefly discussed below. In terms of actual seismic records, only P-wave records are presented herein due to space limitations.

3.1 Triggering Associated with the Hand-Operated Mechanical Source

The basic approach to determine the consistency of source triggering was the same for each source type. The difference between the source types was simply the instruments used to generate the source input. For the conventional, hand-operated mechanical sources, the instant the sledge hammer struck the plate (P waves) or plank (S waves) was determined with a Geometrics hammer trigger securely attached near the head of the sledge hammer. The seismic signal from the hand-operated source was monitored at a fixed, surface location with a 3-D geophone that was buried about 0.15 m into the ground near the borehole as shown in Fig. 1. This 3-D surface geophone is identified as item #4 in Fig.1 and in Table 1.

An example showing three sets of triggering records using the hand-operated P-wave source is presented in Fig.4. The three sets of records are associated with 3-D borehole receiver measurements at depths below grade (DsBG) of 156, 159 and 162 m. (The borehole records associated with these P-wave measurements are presented in Fig.6.) Reference points are shown for: (1) averaged waveforms monitored from the seismic trigger in Fig.4a, and (2) averaged waveforms monitored from the vertical geophone in the 3-D surface geophone in Fig.4b. It should be noted that the reference points are translated to the time axis in Figs.4a and 4b. The reference time for the

(a) Output signal from trigger on
sledge hammer

(b) Output signal from vertical component
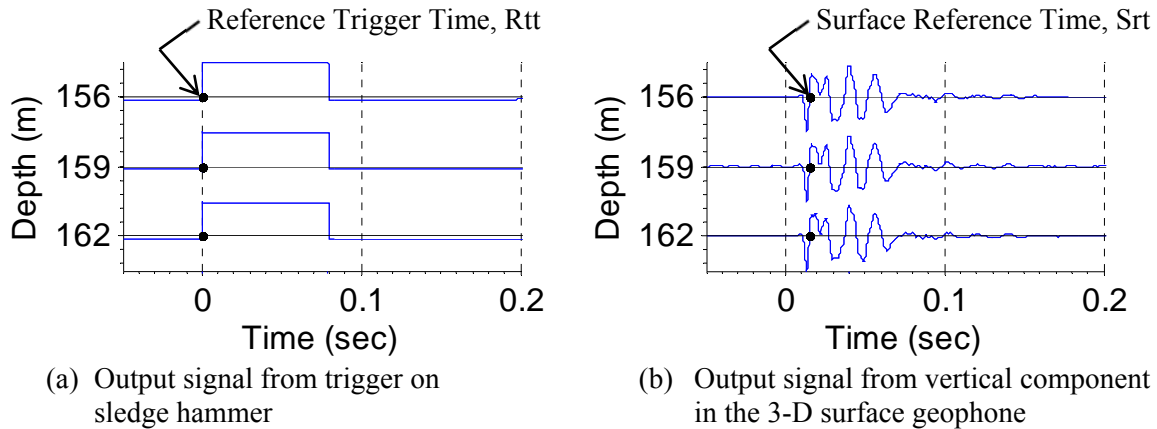in the 3-D surface geophone

Fig. 4 – Examples of the consistency of triggering associated with generating P waves using the hand-operated
seismic source; Records are averaged records from multiple impacts; Depths noted on the vertical axes
are measurements depths associated with the P-wave records presented in Fig.6.

output signal from the trigger is called the reference trigger time and is designated as Rtt in Fig.4a. The reference point for the output signal from the vertical geophone in the 3-D surface geophone is called the surface reference time and is designated as Srt in Fig.4b. These times shown by the reference points are easily and accurately identified, and the reference times in each set of records are identified at the same voltage within that record set and then translated to the time axis. The key point in determining the consistency of triggering is that the time difference between Rtt and Srt remains nearly the same for all measurement depths. This time difference, presented as delta time (Δt), is expressed as:

$$\Delta t = Srt - Rtt \tag{1}$$

As an example of these measurements, consider the records presented in Fig.4. The Δts associated with these measurements are 0.01516, 0.01516 and 0.01523 sec, respectively. The largest difference between the Δts in this set of three records is 0.00008 sec, or slightly less than 0.1 ms. This difference is well within the range needed for consistency of triggering. It is also worth noting that a sampling frequency of 12,800 Hz was used in recording all seismic signals which equates to a sampling Δt of 0.000078 sec; hence, the largest difference in the set of three records in Fig.4 is simply due to the sampling frequency. When all 55 P-wave measurements performed with the hand-operated source are reviewed over the depth range of 18 to 183 m, the maximum Δt is about 0.9 ms and the standard deviation is about 0.2 ms; hence, very good triggering.

3.1 Triggering Associated with the Hydraulically-Operated Seismic Source

When using T-Rex as the seismic source, the consistency of source triggering was based on monitoring the input sinusoidal signal to T-Rex and the output signal from the buried 3-D surface geophone. The input source signal was generated with a function generator. The input source signal triggered T-Rex and was simultaneously sent to the Data Physics recorder as illustrated in Fig.1.

An example showing the consistency of triggering T-Rex for P-wave measurements performed at DsBG of 156, 159 and 162 m is presented in Fig.5. Note that these records are for P-wave measurements performed at the same depths as the records shown for triggering the hand-operated source in Fig.4. This comparison is possible because a 30-m measurement overlap zone was tested using both types of seismic sources. The Δts for the records in Fig.5 are 0.03758, 0.03766 and 0.03750 sec. The different Δt values compared with the hand-operated source is simply due to the distance between the 3-D surface geophone and the source location. The largest difference between the Δts is 0.00016 sec, or slightly less than 0.2 ms. This difference is well within the range needed for

5

(a) Output signal from function
generator used to drive T-Rex

(b) Output signal from vertical component
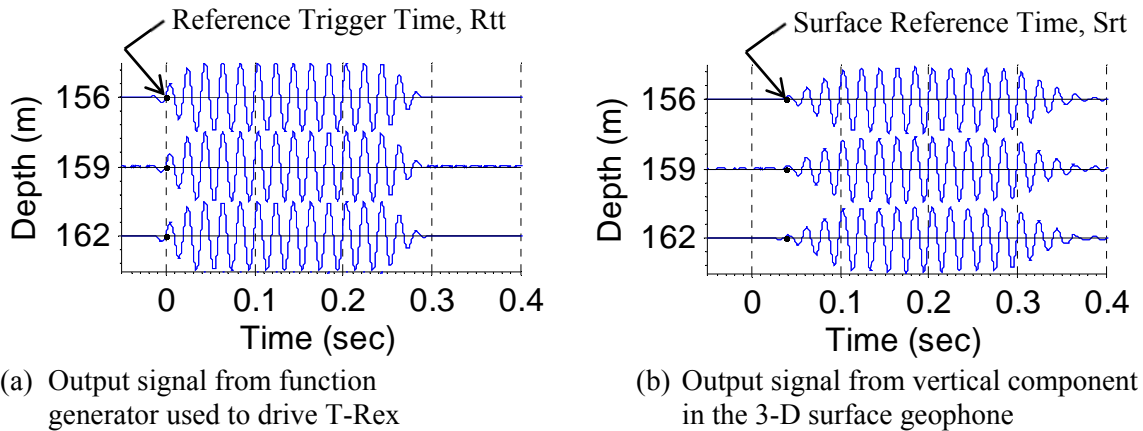in the 3-D surface geophone

Fig. 5 – Examples of the consistency of triggering associated with generating P waves using the hydraulically-operated seismic source (T-Rex); Records are averaged records from multiple shakes; Depths noted on the vertical axes are measurement depths associated with the P-wave records presented in Fig.7.

consistency of triggering. When all 44 P-wave measurements performed over the depth range of 152 to 354 m using the 50-Hz drive signal are considered, the maximum Δt is about 0.5 ms, with a standard deviation of about 0.1 ms; hence excellent triggering.

4. Examples of Time-Domain Records and Data Processing

The P and S waves generated during downhole testing were monitored at depth with one, 3-D borehole geophone as illustrated in Fig.1. The 3-D borehole geophone is identified as item #5 in Fig.1 and in Table 1. This geophone is a Geostuff Model BHG3 triaxial downhole sensor. The 3-D geophone was lowered and raised using a power winch, and the depth was determined with a rotary encoder. Both pieces of equipment are identified as item #6 in Table 1. The borehole geophone also contained an internal fluxgate compass that was used to orient the geophone each time after it was clamped against the casing wall. The compass was useable because the borehole casing is made of stainless steel. The 3-D borehole geophone was oriented each time so that the horizontal geophone element (also called the transverse horizontal geophone) was parallel to the direction of shear wave excitation created by whichever source was being used. Much of this equipment was housed in the Wireline Van shown in Fig.1.

4.1 P- Wave Records Using the Hand-Operated Seismic Source

A set of 3, unfiltered ("raw") P waveforms recorded at DsBG of 156, 159 and 162 m is presented in Fig.6a as an example of the field data. These waveforms were filtered in the laboratory with a 50-Hz, low-pass, digital, filter before they were used to identify a reference point on each waveform. As seen in Fig.6a, these records contain some noise that should be removed to aid the analysis procedure. The unfiltered, time-domain signals were transformed into the frequency domain using the discrete Fast Fourier Transform (FFT). A 50-Hz, low-pass filter was applied by multiplying the filter coefficients with both the real and imaginary parts of the frequency magnitudes to obtain a modified frequency response. Then, the inverse FFT was performed on the modified frequency response to obtain a filtered signal in the time domain as shown in Fig.6b.

The unfiltered P-wave records in Fig.6a contain a strong and identifiable P-wave arrival. However, the filtered records in Fig.6b are even easier to identify and track with depth so these records were used in the analysis phase. A reference point on the P waveforms using the first large peak was selected. This point is designated as the borehole reference point (Brp) in Fig.6b and was selected using waterfall plots with generally 8 or more

6

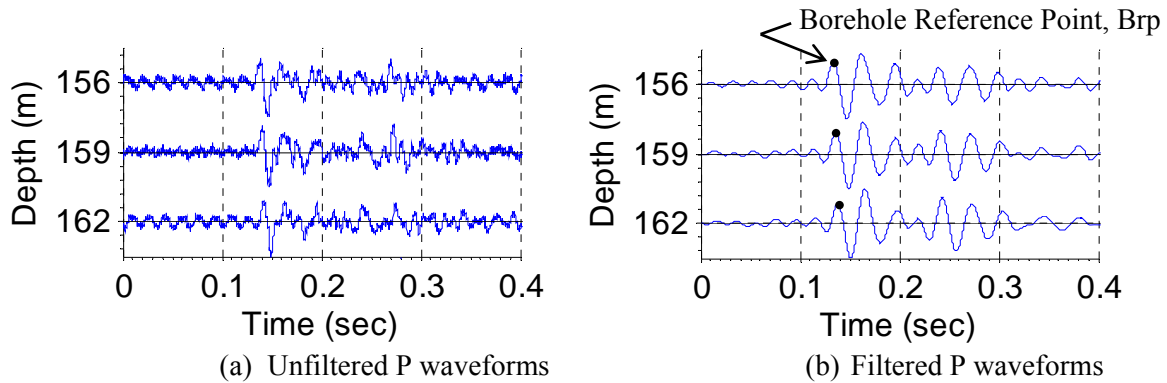(a) Unfiltered P waveforms   (b) Filtered P waveforms

Fig.6 – Examples of unfiltered and filtered P waveforms generated with the hand-operated seismic source; Measurement depths of 156, 159, and 162 m in the borehole; Voltage in each time record is normalized to a maximum value = 1.0.

waveforms that exhibited continuity in the waveform shape over substantial depths. Since the waveform shapes containing frequencies below 50 Hz remained nearly the same over substantial depths, the filtering had essentially no effect on relative travel times determined from the travel time versus depth plots (Stokoe et al., 2016 [2]). The reference Brp points on the filtered P waveforms in Fig.6b are surrogates for wave arrivals from which arrival times are determined as discussed in Section 5.

4.2 P-Wave Records Using the Hydraulically-Operated Seismic Source

As done with hand-operated seismic source, unfiltered ("raw") P waveforms generated with T-Rex were filtered in the laboratory with a 100-Hz, low-pass, digital, filter before they were used to identify a reference point on each waveform. A set of 3 unfiltered P-wave waveforms recorded at DsBG of 156, 159 and 162 m is presented in Even though these records contain little noise, the filtered records, presented in Fig.7b, were easier to identify and track with depth so these filtered records were used in the analysis phase. All other processing of these waveforms generated with T-Rex was the same as described in Section 4.1

5. Waterfall Plots, Relative Travel-Time Plots and Interpreted Wave Velocities

Waterfall plots of the filtered waveforms were used to determine consistent reference points with depth as shown in Fig.8. It should be noted that the filtered waveforms in the waterfall plots were first scaled (amplified) according to depth squared before the reference points were picked. The first large peak in the scaled P waveform, the Brp, is a surrogate for the P-wave arrival. The borehole reference points are identified by the red circles on the waveforms in Fig.8. Once the Brps were picked, the times associated with the Brps were identified on the time axis. These reference times are designated as borehole reference times (Brts) and are identified by the black circles on the time axis in Fig.8. The Brts were then used in the waveform waterfall plots so that these plots could be studied and zones of constant velocity could be identified. In this case, an initial linear regression line was fit to the data simply as a guide in identifying zones of constant velocity but realizing that actual velocities need to be evaluated from times of vertically propagating waves as discussed below.

The final step in determining the P-wave velocities of individual layers was to adjust the P-wave travel times (Brts) shown in Fig.8 to travel times of vertically propagating P waves. This step involved: (1) assuming a straight ray path for the inclined P wave from the surface source to the 3-D borehole geophone, (2) calculating the inclined source- to-receiver distance, and then (3) multiplying the travel times (Brts) by the ratios of the vertical depths divided by the inclined travel-path lengths. (This adjustment is equivalent to multiplying the travel times by the cosine of the angle between the vertical path and the straight-line slant path from the source to the receiver.) In the

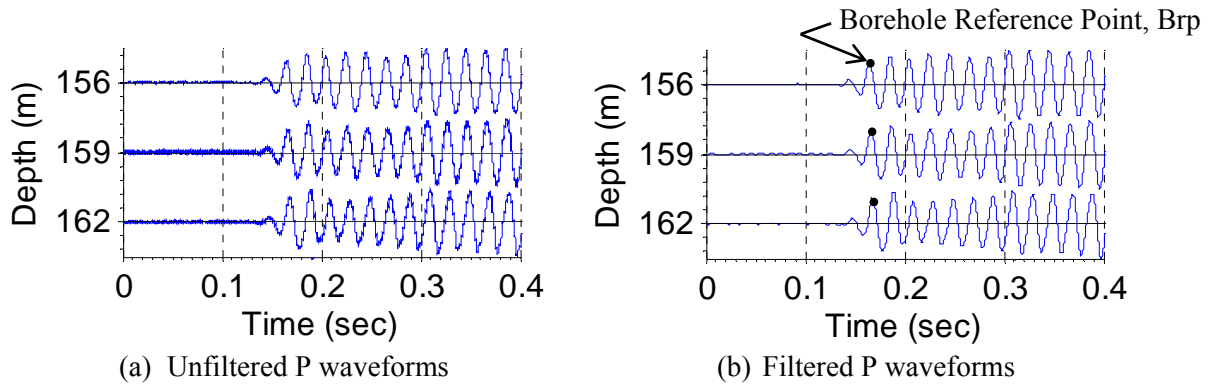(a) Unfiltered P waveforms   (b) Filtered P waveforms

Fig. 7 – Examples of unfiltered and filtered P waveforms generated with the hydraulically-operated seismic source; Measurement depths of 156, 159, and 162 m; Voltage in each time record is normalized to a maximum value = 1.0.
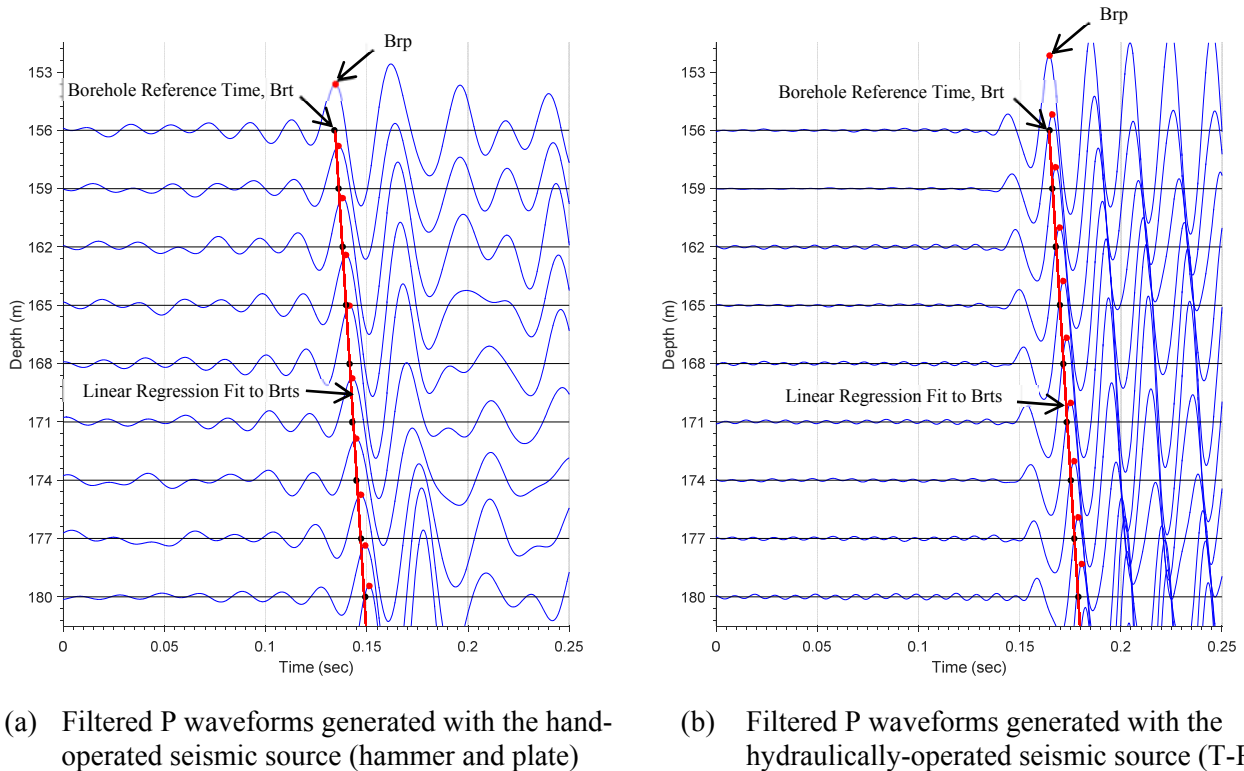

(a) Filtered P waveforms generated with the hand-operated seismic source (hammer and plate)

(b) Filtered P waveforms generated with the hydraulically-operated seismic source (T-Rex)

Fig.8 – Example scaled waterfall plots of filtered P waveforms from the vertical receiver in the 3-D borehole geophone; Testing depths of 156 to 180 m; Travel-time "picks" (Brts) are shown on the time axis (black circles); Initial linear regression line (red line) fit to the Brts indicate a zone of constant velocity.

calculations of the "adjusted travel times", the assumption is also made that any refraction of the P wave that may have occurred is insignificant since the inclined ray paths are already nearly vertical. The adjusted travel times were then plotted versus depth. This plot is shown in Fig.9a for the combined P-wave measurements with both source types. The adjusted travel times are represented by the data points at 3-m intervals over DsBG of 18 to 183 m for the hand-operated source. For the T-Rex source, the adjusted travel times are represented by data points at 3-m intervals over DsBG of 152 to 183 m and then 6-m intervals over DsBG of 189 to 415 m. Linear regression
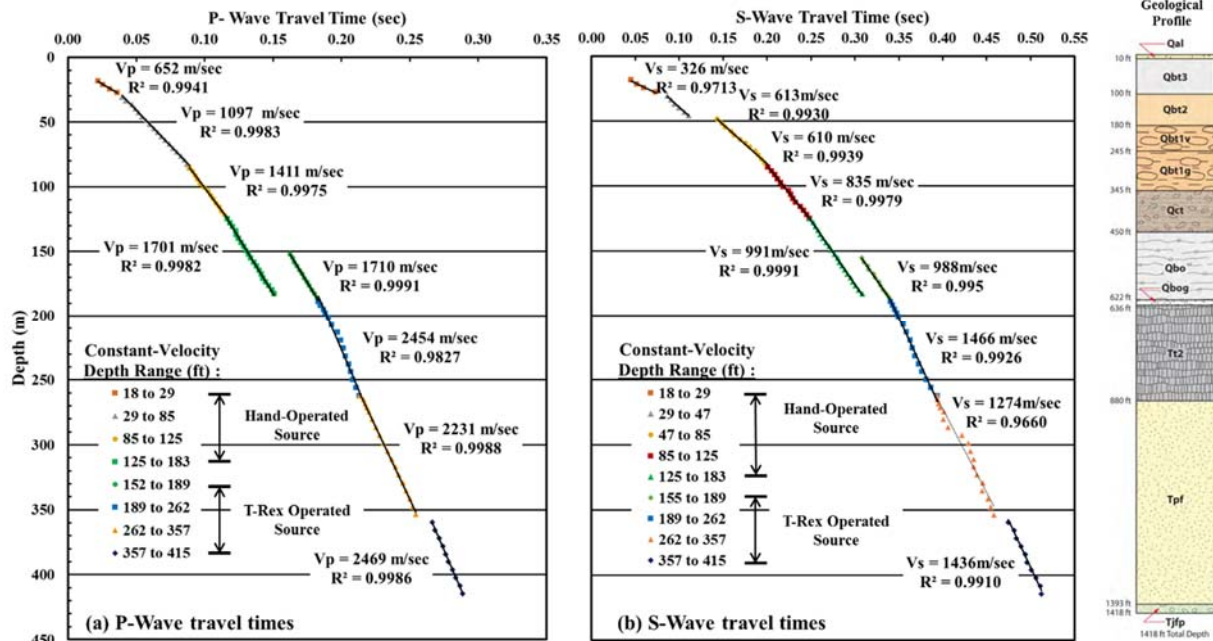
8

Fig. 9 – Composite P-wave and S-wave travel-time plots for measurements with both types of seismic sources over depths ranging from 18 to 415 m.

lines were fit independently to each set of data points to create constant-velocity layers. Each linear regression line has the form:

$$y = V * x + c \qquad (2)$$

where x is the travel time of a vertically propagating wave, V is the wave velocity, y is the vertical depth below the ground surface, and c is the depth intercept at zero time. In this case, V equals the P-wave velocity of the layer being analyzed. In Fig.9a, layer depths were estimated to the closest 1.5 m at depths to 200 m and to the closest 3 m at depths below 200 m. Also, the coefficients of determination, R^2, of the linear-regression fits are presented. In every case, the values of R^2 are greater than 0.994. These R^2 values, combined with "by-eye" checks, indicated excellent fits to the data.

Determination of the S-wave velocities followed the same analysis procedure used to determine the P-wave velocities. The S-wave travel-time plot for the combined measurements with both sources is presented in Fig.9b. Linear regression lines were fit independently to the S-wave data from each source type. In five of the seven constant-velocity layers, the R^2 values were above 0.990. These values and "by-eye" checks indicated an excellent fit to the data. For the shallowest layer (DsBG of 18 to 29 m) and a deeper layer at DsBG of 262 to 357 m, the R^2 values were around 0.970. The "by-eye" checks of these linear fits indicated very reasonable fits to the data.

It is also interesting to compare the V_P and V_S values determined with each source type over the depth range of 153 to 183 m. In this over-lap zone where testing was performed with both source types, the V_P values are within 0.5 % (Fig.9a), and the V_S values are within 0.3 % (Fig.9b). Hence, excellent agreement was obtained between the traditional and higher-energy testing methods.

Composite V_P and V_S profiles determined at the borehole are presented together in Fig.10. Both profiles have been divided into seven, constant-velocity layers. The commonality in velocity layering occurred, for the most part, through a few minor adjustments to the layer boundaries that were agreed upon by UT and LANL personnel during the analysis stages. It is also interesting to note that the wave velocities in Fig.10 exhibit a general correlation with the material profile in the geological profile shown on the right-hand side of the figure. However,

the correlation is rather poorly defined in the depth range of 55 to 137 m. The reason or reasons for this zone of poorer correlation remain to be investigated in future work.

The resulting profile of calculated values of Poisson's ratio, ν, versus depth is presented along with the V_P and V_S profiles in Fig.10. The values of ν were calculated from:

$$\nu = \left(2 - \left(V_P/V_S\right)^2\right) \Big/ \left(2 - 2 * \left(V_P/V_S\right)^2\right) \qquad (3)$$

The values of ν range from 0.222 to 0.333, with the largest value of 0.333 occurring in Layer #1 with material having V_S less than 335 m/s. Once V_S equals or exceeds 765 m/s, the values of Poisson's ratio range from 0.222 to 0.258; quite reasonable values for tuff materials that exist in most of the geological profile in Fig.10.

6. Alternative Profiles and Evaluations of the Profiles

Two alternative solutions to the P- and S-wave velocity profiles were developed in which modifications to the profiles seemed as reasonable or nearly as reasonable as the original fittings of the P-wave and S-wave travel time versus depth plots that are shown in Fig.9. Of course, it is to be expected that the alternative solutions would likely result in only small changes in portions of the overall velocity profiles because the solutions presented in Fig.9 are quite robust based on: (1) the high values found for the correlation coefficients, (2) the robustness of the correlations based on the "by eye" checks, and (3) the reasonable values of Poisson's ratio. Generally, values of R^2 are above 0.990 for each linear segment in the travel-time plots. The reasonableness of alternative velocity profiles were "judged" by comparing the total travel times, from top-to-bottom of the geologic column being considered, determined from: (1) the alternative profile, (2) the original profile (Figs.9 and 10), and (3) the field measurements. Values of Poisson's ratio calculated with the V_P and V_S values were also considered in terms of judging the reasonableness of the alternatives. Each alternative is briefly discussed due to space limitations.
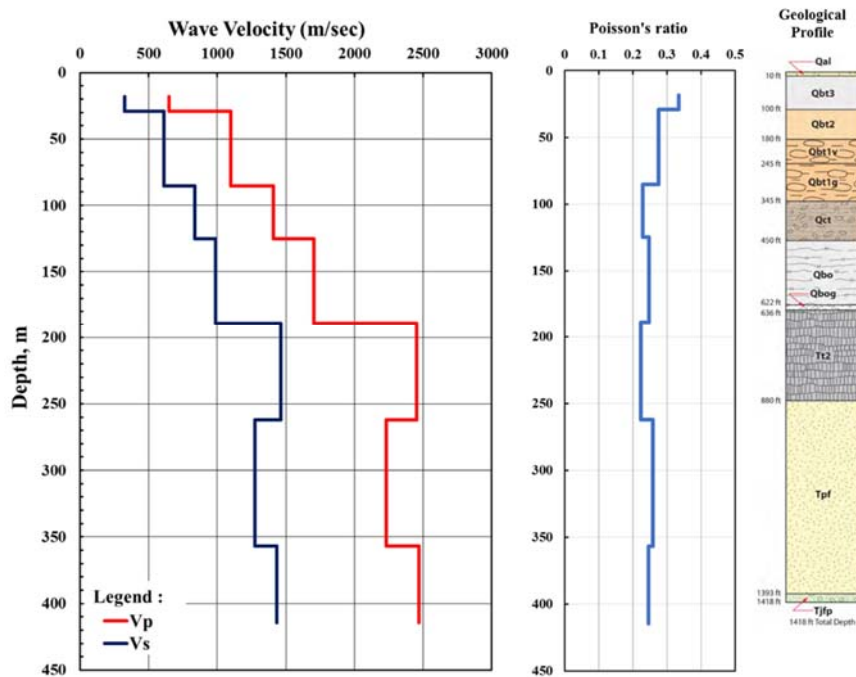

Fig.10 – Composite V_P and V_S profiles determined at the LANL deep borehole and the resulting profile of calculated values of Poisson's ratio.

The first set of alternative V_P, V_S and ν profiles consists of re-evaluating the travel-time measurements with the hand-operated sources over the depth range of 18 to 183 m while leaving the remainder of the profiles in Fig.10 unchanged. The change to the original P-wave profile in Fig.10 was to move one interface, the one between Layers #2 and #3, from a depth of 85 m to a shallower depth of 76 m as shown in Fig.11. The resulting changes are that the P-wave velocity in Layer #2 decreased by about 2 %, from 1098 m/s to 1077 m/s, and the P-wave velocity in Layer #3 increased by about 1 %, from 1412 m/s to 1424 m/s. The values of R^2 increased slightly (less than 0.15 %) in both cases. The value of the calculated total travel time over the depth range of 18 to 183 m for the alternative P-wave velocity profile is closer to (0.29 % smaller) the top-to-bottom field measurement of 128.95 ms than the calculated total travel time for the original P-wave profile (0.70 % larger). Hence, the alternative profile is just as reasonable or slightly better than the original profile.

The associated S-wave measurements in Fig.10 over the depth range of 18 to 183 m in the first set of alternative profiles was more involved. The first change in the measurements was to move the interface at 85 m to a shallower depth of 76 m, just as was done with the alternative P-wave profile. The second change was to add another layer boundary at 48 m which created an addition S-wave layer in the depth range of 48 to 76 m as shown in Fig.11. The value of the calculated total travel time over the depth range of 18 to 183 m is closer (0.42 % larger) to the top-to-bottom field measurement of 229.33 ms than the calculated total travel time for the original S-wave profile (0.75 % larger). Hence, the alternative profile is just as reasonable as the original profile. Furthermore, the Poisson's ratio profile in Fig.11 is also quite reasonable. The result is that the first set of alternative profiles are judged to be as reasonable as the original set of profiles. Hence, these profiles are given equal weight.

The second set of alternative V_P, V_S and ν profiles is presented in Fig.12. The adjustments to this set of profiles is more complex than the first set of alternative profiles and, due to space constraints, cannot be explained in detail. One important difference is that a high-velocity layer (a layer of dacite) around a depth of 245 m could be interpreted, particularly on the P-wave measurements. Therefore, this and other changes were made. The second set of alternative profiles were also given a weight equal to each of the other two sets of profiles.
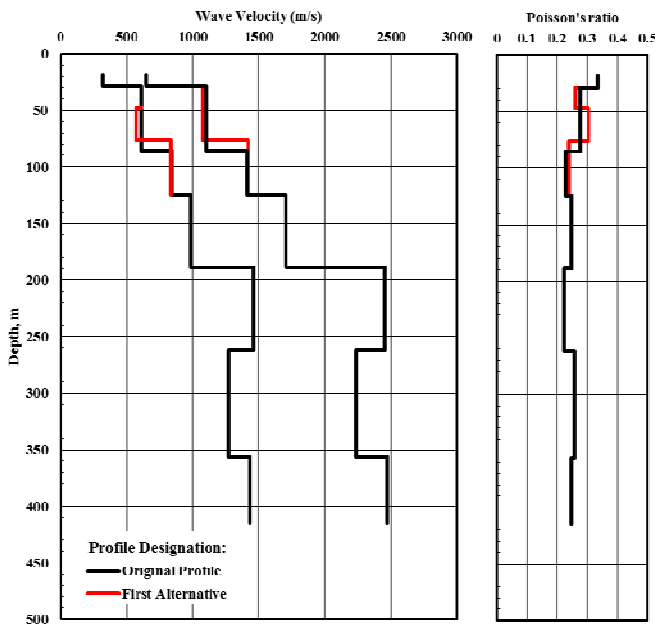

Fig.11 – Comparison of the original set of V_P, V_S and ν profiles with the first alternative set of V_P, V_S and ν profiles.
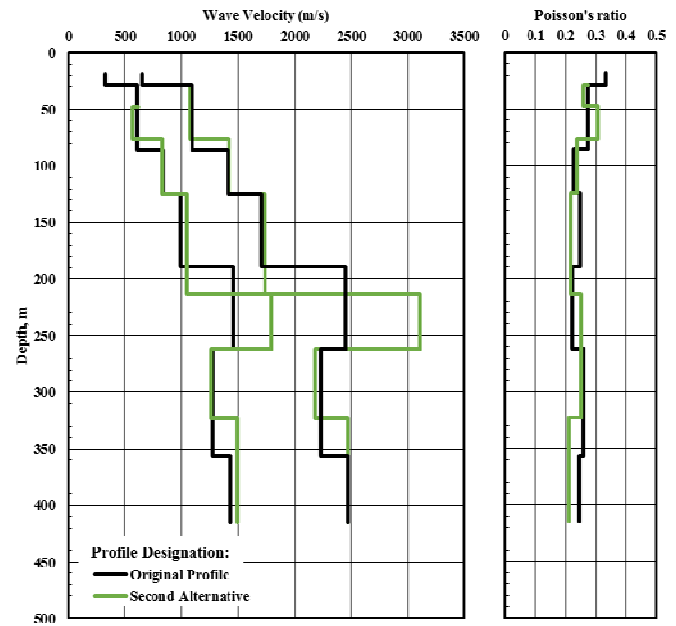
Fig.12 – Comparison of the original set of V_P, V_S and ν profiles with the second alternative set of V_P, V_S and ν profiles.

7. Summary and Conclusions

Deep downhole seismic testing was performed in an existing borehole at the LANL site. Two types of seismic sources were used. Hand-operated seismic sources (sledge-hammer and plate for P-wave measurements and sledge-hammer and plank for S-wave measurements) were used over the depth range of 18 to 183 m. Robust P and S waveforms were generated with both source types. In both cases, filtering the waveforms assisted in identifying key points on the waveforms used to determine travel times.

The second seismic source type was a hydraulically-operated, controlled-waveform source, named T-Rex. In this work, the multi-directional shaking capability of T-Rex was used; hence, vertical shaking for P-wave measurements and longitudinal (horizontal) shaking for S-wave measurements. In each shaking direction, T-Rex was operated as a fixed-frequency source with 10 full-amplitude cycles of shaking. For testing over the depth range of 150 to 354 m, a 50-Hz drive signal was used. The drive signal was then changed to 30 Hz to improve signal clarity and this drive signal was used over depths of 360 to 415 m. As done with the P and S waveforms generated with the hand-operated sources, filtering was performed to assist in identifying key points on the waveforms. Also, a 30-m thick zone (depths of 152 to 183 m) existed where measurements were performed with both types of sources. In this zone of overlapping measurements, the values of V_P and V_S determined with both types of sources agreed well, with differences less than 0.5 %.

The original V_P and V_S profiles determined at the deep borehole are presented in Fig.10. Both velocity profiles were divided into seven, constant-velocity layers. The commonality in velocity layering occurred, for the most part, through a few minor adjustments to layer boundaries. The V_P profile was first analyzed and, as expected, contained the more robust and simpler time records. The resulting profile of Poisson's ratio, ν, versus depth was determined using the V_P and V_S profiles.

The reasonableness of this original set of V_P and V_S profiles was confirmed by good agreement between calculated and measured total travel times for both the P and S waves. The calculated total travel time is within 0.55 % of the measured total travel time in the field for V_P. The same comparison for V_S is 1.92 %. The robustness of both the V_P and V_S profiles is further supported by the reasonable values in the Poisson's ratio profile. Two alternative V_P, V_S and ν profiles, presented in Figs.11 and 12, are also briefly discussed. These sets of profiles perform equally as well in terms of reasonableness and calculated total versus field-measured travel times and are given equal weight to the original set of profiles.

8. Acknowledgements

9. References

[1] Stokoe, K.H., II, Li, S., Cox, B., Menq, F-Y, and Rohay, A. (2008), "Deep Downhole Seismic Testing for Earthquake Engineering Studies", Proceedings, 14th World Conference on Earthquake Engineering, 12-17, Beijing, China.

[2] Stokoe, II, K.H., Hwang, S., Roberts, J.R., Menq, F. M. and Keene A.K. (2016), "Deep Downhole Seismic Testing at LANL Using T-Rex as the Seismic Source; P- and S-Wave Measurements in Boreholes R-25C and R-60, Volumes I of II; Summary of Seismic Tests and Wave Velocity Profiles," Geotechnical Engineering Report GR15-04, Geotechnical Engineering Center, Civil Engineering Department The University of Texas at Austin, 342 p.